DESIGN OF DIFFRACTIVE ELEMENTS AT MILLIMETER WAVELENGTHS USING SUBWAVELENGTH CYLINDRICAL MICROSTRUCTURES

Mark S. Mirotznik,[1] Timothy Creazzo,[2] and Scott Mathews[1]
[1] Department of Electrical Engineering and Computer Science, The Catholic University of America, 620 Michigan Ave NE, Washington, DC 20064
[2] Department of Electrical and Computer Engineering, The University of Delaware, Newark, DE 19716

Received 24 January 2007

ABSTRACT: *We describe a design methodology for synthesizing diffractive elements based on two-dimensional subwavelength cylindrical microstructures. We combine a numerical and experimental approach to demonstrate that by varying the diameter, pitch, and depth of subwavelength cylindrical occlusions in a homogenous substrate it is possible to produce multiphase diffractive elements.* © 2007 Wiley Periodicals, Inc. Microwave Opt Technol Lett 49: 1880–1884, 2007; Published online in Wiley InterScience (www.interscience.wiley.com). DOI 10.1002/mop.22571

Key words: *diffractive; subwavelength; rigorous couple wave; millimeter wave and effective media*

1. INTRODUCTION

Phase-only diffractive elements (DEs) are an attractive technology for a variety of applications at optical, millimeter wave and microwave frequencies, where arbitrary wavefront generation is desired. The DE's small size and ability to generate complex wavefronts contributes to its popularity, particularly for applications involving monochromatic illumination. Most DEs are designed using algorithms based on scalar diffraction theory and are fabricated with large features relative to the operational wavelength. Unfortunately, at longer wavelengths the size of scalar domain features tends to be sufficiently large as to prohibit the fabrication of a practical DE that meets size and weight constraints. Over the last decade several investigators have developed techniques for constructing subwavelength DEs using effective media theory [1–4]. These devices are capable of producing quite general phase profiles, including polarization dependant phase profiles. In particular, we recently described a design methodology for synthesizing polarization-sensitive diffractive optical elements based on 2D form-birefringent microstructures and a cell-encoding design algorithm [4]. That technique yielded a single-substrate binary element that generated nearly independent phase responses for horizontally and vertically polarized illumination. That method was demonstrated experimentally at long-wave infrared and was shown to be effective.

In this article, we extend the subwavelength cell-encoding procedure described in [4] to include subwavelength features that are cylindrically shaped (as shown in Fig. 1). The advantage of using cylindrically shaped subwavelength features is that inexpensive fabrication processes such as conventional mechanical or laser drilling can be employed for DE fabrication. We also extend the concept of subwavelength DEs to longer millimeter wavelengths. Several elements were fabricated using conventional mechanical drilling, based on the design process described in this article and characterized at millimeter wavelengths (~40 GHz).

2. DESIGN METHODOLOGY GENERAL CONCEPT

Phase-only DEs are designed by mapping an electromagnetic wave's phase function into a surface relief pattern. Typically, the phase function is realized by modulating the height of an area whose dimensions are fixed for each phase value. (This technique is referred to as point-oriented encoding.) If the dimensions of the diffracting feature are much larger than the illuminating wavelength, the phase transformation is insensitive to polarization. The degree of phase transformation is simply given as, $\nabla\phi = (2\pi d/\lambda_o)(n-1)$, where, d is the height of the dielectric feature, n is the index of refraction of the substrate and l_0 is the free-space wavelength. If instead a periodic array of subwavelength features is used then the degree of phase transformation is determined by the "effective" index of refraction of the subwavelength grating (i.e. $\nabla\phi = (2\pi d\lambda_o)(n_{\text{eff}} - 1)$). The effective index is a relatively sensitive function of the grating's period, feature shape, and thickness, as well as the bulk electromagnetic properties of the isotropic substrate. Thus, a large number of design parameters can be exploited in designing subwavelength DEs. Additionally, subwavelength gratings will respond anisotropically if either the grating periods (Λ_x and Λ_y) or feature shape differs along the x- and y-directions. This opens up the possibility of synthesizing polarization-dependent DEs.

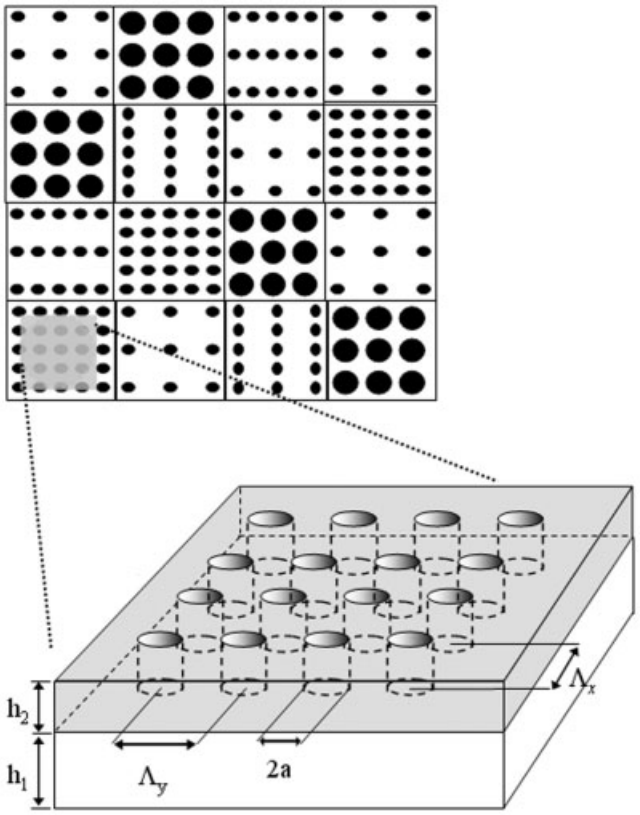

Figure 1 Schematic representation of a sub-wavelength DE with cylindrical features. Each cell location produces an effective electromagnetic property as a function of the x- and y-grating periods, hole-diameter, and grating depth

In [4] a design algorithm was presented that utilized a look-up table of effective properties as a function of the grating's parameters as building blocks to synthesize more complicated DEs. The effective properties were precalculated using the rigorous coupled wave (RCW) method and used to generate more complicated, spatially varying DEs. To insure that each grating generates only a 0th diffractive order in both transmission and reflection, the grating periods, Λ_x and Λ_y, were restricted to less than λ_0, where λ_0 is the free-space wavelength of illumination. Furthermore, to

simplify fabrication and modeling, only binary rectangular gratings were studied in [4]. For this article, we use the RCW method to calculate the effective electromagnetic properties generated by varying the radius (a), height (h), and grating periods (Λ_x, and Λ_y) of cylindrical subwavelength features (shown in Fig. 2). A look-up table design approach, similar to the approach described in [4], was used to cell-encode the phase function of more general DEs.

2.1. Effective Properties of Two-Dimensional Subwavelength Gratings With Cylindrical Features

Two approaches are generally reported in the literature for determining the effective optical properties of subwavelength gratings. The first uses closed form expressions [5] to provide approximate effective phase values as a function of the grating structure. Although attractive from a computational perspective, the approximate expressions are accurate only for gratings whose period is much smaller than the wavelength of illumination. Additionally, as the grating period approaches the wavelength, which is referred to as the resonance regime, the assumptions on which these closed form expressions are based are no longer valid.

We employ a second approach, which utilizes a rigorous electromagnetic model to determine the relationship between structural form and response. Although computationally more difficult, the approach is capable of generating accurate results for gratings of any period size and shape. Several rigorous electromagnetic models can be used for this calculation. We chose the RCW algorithms because they offer the best compromise between accuracy and computational expense. To this end, we developed a rigorous model based on the method described by Noponen and Turunen [6] to calculate the effective electromagnetic properties of two-dimensional subwavelength gratings with cylindrical features. For brevity the mathematical details of the RCW method are not described here. For a detailed description the reader is referred to [6, 7].

The geometry of our structure, represented in Figure 2, is composed of a binary surface relief pattern with cylindrical features, a homogenous slab of finite thickness, and two semi-infinite dielectric media denoted as the incident and transmission regions. The illumination from the incident region is assumed to be normally incident on an isotropic homogenous slab of refractive index n_h and thickness h_1 ($0 < z < h_1$). The grating layer fills the next region defined by $h_1 < z < h_2$ and is composed of a two-dimensional periodic array of cylindrical features. Within the grating layer, the index of refraction is modulated between the substrate refractive index n_s and the refractive index of the cylindrical features, n_c. We denote the incident region as a semi-infinite space in which $z < 0$ and the transmission region as a semi-infinite space in which $z > h_2$. We assume both semi-infinite regions are filled with free-space, $n_0 = 1$. The incident field is a plane wave, linearly polarized in the xy-plane and propagating in the $+z$ direction,

$$\vec{E}_{\text{inc}} = \widehat{u}\, E_0 e^{-jk_s z} \tag{1}$$

where $\widehat{u}$ is a unit vector in the direction of polarization, E_0 is the amplitude, and k_s is the wavenumber of the incident region. The RCW described in [6] calculates all transmitted and reflected orders diffracted by the subwavelength grating shown in Figure 2. Of primary interest here are the amplitudes of the transmitted diffractive orders $T_{\text{m,n.}}$ Specifically, if the grating periods are constrained to be less than the free-space wavelength, i.e., Λ_x, $\Lambda_y < \lambda_0$, only the 0th order transmitted order, represented by $T_{0,0}$, propagates. The relative phase lag introduced by the subwavelength grating is easily determined from $T_{0,0}$ as,

$$\nabla\phi = \angle T_{0,0} - k_0 h_2, \tag{2}$$

where $\angle T_{0,0}$ denotes the angle of $T_{0,0}$ and k_0 is the free-space wavenumber. From Eq. (2), the effective index of refraction for the grating can be determined as $n_{\text{eff}} = (\lambda_0/2\pi h_2)\,\nabla\phi + 1$. It should be noted that the concept of this being an effective electromagnetic medium is only approximate, and therefore strictly valid only for the case of normal illumination at a specific wavelength. However, for the case of interest here (i.e. designing a phase-only DE), we are concerned only with the 0th order relative phase lag generated by the subwavelength grating under normal illumination. A RCW code, as described in [6, 7], was written in the programming language MATLAB™ to solve for the effective electromagnetic properties of subwavelength cylindrical gratings.

2.2. Results of Effective Properties

The RCW method was used to generate tables of effective properties for the geometry illustrated in Figure 2. For the designs examined in this study it was assumed that the cylindrical holes were drilled into a nearly lossless dielectric plate of polystyrene (Rexolite™). Consequently, we fixed a constant total thickness of the homogenous slab + grating (h_2), the wavelength of illumination, and all dielectric constants. The radius of the cylindrical holes (a), the periods (Λ_x and Λ_y), and thickness of the grating layer ($h_2 - h_1$) were assumed variable. Figures 3(a)–3(c) illustrates typical results for the effective phase variation that can be achieved by subwavelength gratings with cylindrical features. For these examples the thickness of the plate was fixed at $h_2 = 0.5$ in. and the index of refraction of the substrate (Rexolite) was held constant at $n_s = 1.59$. This plate thickness corresponds to roughly a 2π maximum phase variation at 40 GHz, $h \approx (\lambda_0(n_s - 1))$. The results illustrate that relatively large variations in phase can be achieved by varying the hole-diameter and period from 10 to 60% of the material wavelength and varying the grating-depth from 50 to 150% of the material wavelength.

2.3. Cell-Encoded Subwavelength Diffractive Elements

To design DEs with spatially varying effective properties a cell-encoding scheme was employed. In this process a DE with a desired continuous phase response was approximated by a number of finite size cells (as illustrated in Fig. 1). Each cell is assigned a single desired phase value. Given the look-up tables of effective properties, described in the previous section, it is relatively straightforward to identify a grating structure (i.e. hole-diameter,

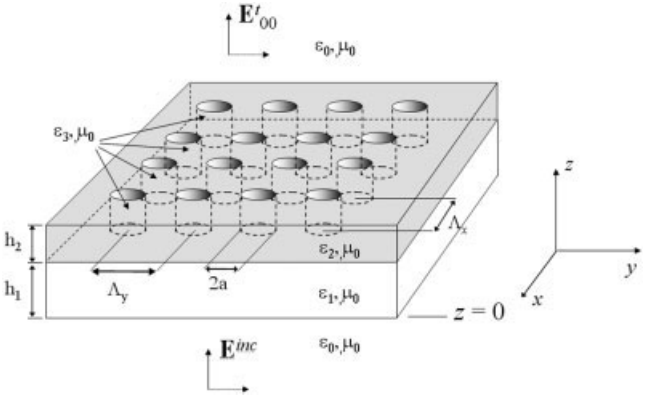

Figure 2 Geometry used to calculate effective properties of sub-wavelength gratings with cylindrical features

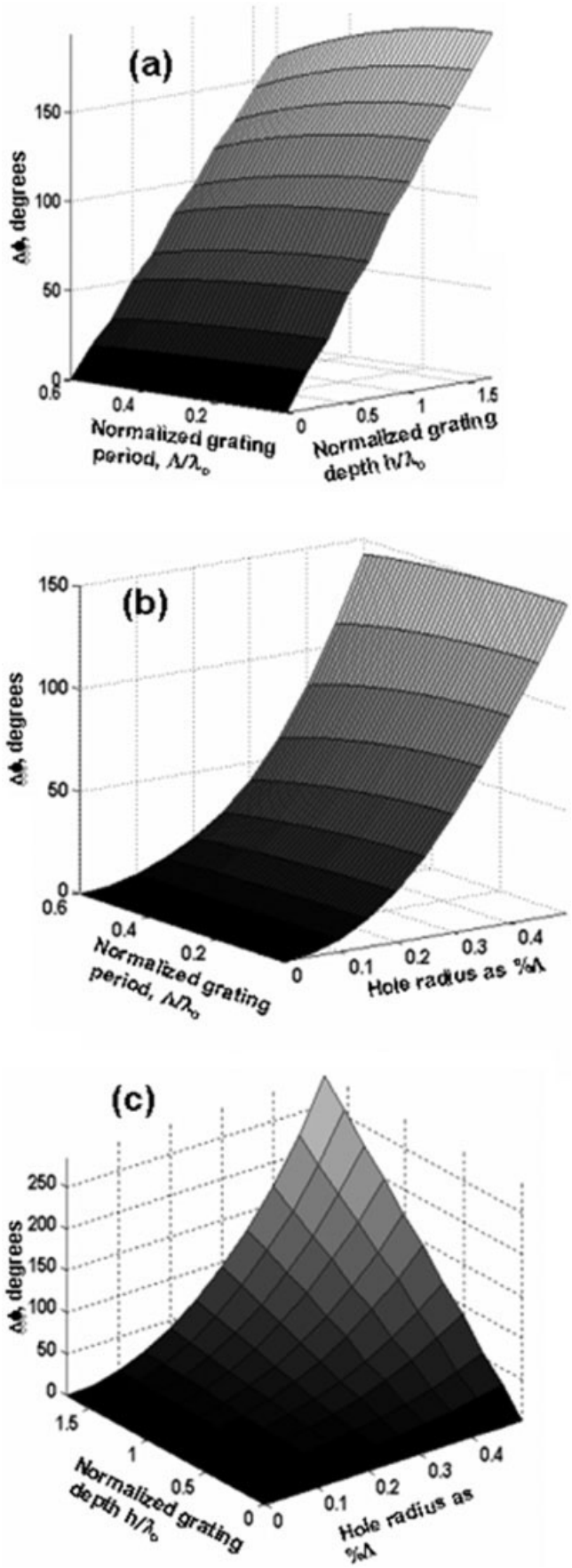

Figure 3 Effective phase transmission as a function of the hole radius, normalized grating period (Λ/l_0), and normalized grating depth (h/l_0). (a) hole radius fixed at 30% of the grating period (b) normalized grating depth (h/l_0) fixed at 0.5, (c) normalized grating period (Λ/l_0) fixed at 0.5

hole–depth, and period) at each cell that most closely matches the desired phase response at that location. It is important that the phase profiles are sampled on a scale larger than the wavelength. From trial and error we found that the phase profiles sampled as frequently as every five material wavelengths produce good results. If the sampling distance is much smaller than this, the number of periods in the subwavelength grating is insufficient to generate the predicted effective electromagnetic properties. Conversely, if the sample distance is too large, the super-wavelength phase profiles do not adequately represent the desired transformation. It should be noted that by restricting the look-up tables to only those grating geometries that can be easily fabricated, we have consequently integrated fabrication constraints into the design algorithm.

3. EXPERIMENTAL VALIDATION

To validate this method we designed, fabricated, and tested two DEs using the method described in Section 2, for operation at a frequency of 40 GHz (Figure 4). One element generated a one-dimensional linear phase ramp from 0° to 210°, while the other element generated a two-dimensional linear phase ramp also from 0° to 210°. Both elements were fabricated by drilling 2.0-mm diameter air holes in a 210 mm × 210 mm × 12.7 mm Rexolite plate using a computer numerical controlled (CNC) milling machine. For ease of fabrication the hole-diameters were fixed at 2.0 mm while the grating depth and period were varied. By fixing the hole-diameter the entire element could be fabricated in a few hours, without changing drill bits.

The fabricated elements were characterized using the experimental set-up shown in Figure 5. In this set-up the machined Rexolite plate was mounted perpendicular to a collimated, millimeter wave source operating at 40 GHz. It has been found from previous studies that this source produces quasi-plane wave fields, whose phase fronts vary by less than 5% over the aperture size of interest. To measure the transmitted complex field values, a small monopole antenna, aligned parallel to the polarization axis of the electric field, was scanned in 1.0 mm spatial increments over a square region (20×20 cm^2) at the center of the Rexolite plate. The probe was placed at a z-distance of ~5 cm from the backside of the DE. We found that this distance was large enough to ensure that the probe did not significantly couple to evanescent fields and small enough to ensure that the results were not corrupted by diffraction artifacts from the outer edges of the Rexolite plate. An Agilent 85106D Vector Network Analyzer was used to provide both a 40-GHz input source as well as measure the phase and magnitude of the transmitted fields at each location of the detector. A computer program, written in Labview™, was used to move the probe, control the network analyzer, and store the results. From the recorded phase angle of the measured transmission coefficient the spatially varying phase lag and effective properties of the sample can easily be determined using Eq. (2).

3.1. One-Dimensional Linear Phase Ramp Results

We designed our first element such that the phase angle of the 0th order transmitted field, at normal incident, varies linearly from 0° to 200°, only along the x-axis. The device was designed in Rexolite ($n_s = 1.59$) for operation at 40 GHz. At 40 GHz, the plate thickness of 12.7 mm corresponds to a phase delay slightly larger than 2π. To employ the cell-encoding algorithm the element, illustrated in Figure 4(a), was divided into a 10×10 array of cells each ~21 mm on a side. Each unit cell was composed of five subwavelength grating periods, with a hole-diameter of 2 mm.

Simulated and experimental results, shown in Figure 6, demonstrate the expected behavior of the device. The results shown are

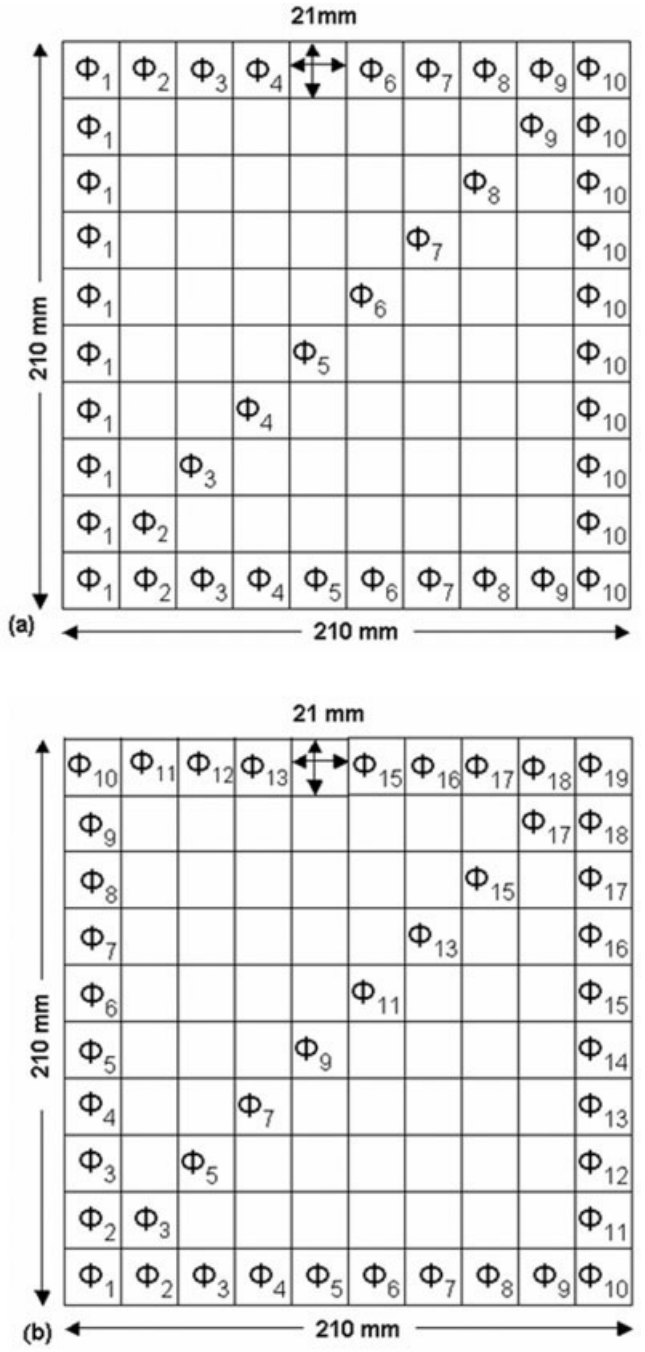

Figure 4 Diffractive elements designed using the cell-encoding algorithm. Each cell is composed of a 5 × 5 array of sub-wavelength gratings with cylindrical features, (a) a 10 × 10 array of cells in which the phase varies linearly along the *x*-axis from 0° to 200°. (b) a 10 × 10 array of cells in which the phase angle varies linearly along both the *x* and *y* -axis from a minimum of 0° (left hand bottom corner) to 200° (right hand top corner)

for a linear scan along the *x*-axis with the probe positioned in the middle of the *y*-axis dimension. Both the experimental and simulated results reveal the expected linear increase in phase from 0° to 200° as the measurement probe is scanned along the *x*-axis. Contained within the measured results are clear phase deviations as large as ±15° about the expected values. We believe that this is most likely caused by random phase uncertainty in the measurement. To test this conjecture we inserted a flat polished Rexolite plate, same thickness as the DEs, into the measurement system and obtained a phase result that also varied randomly as much as ±15°.

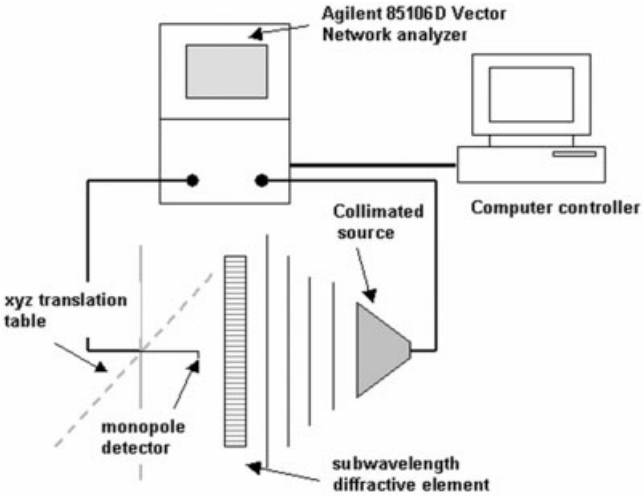

Figure 5 Experimental setup used to characterize the sub-wavelength DEs

3.2. Two-Dimensional Linear Phase Ramp Results

A second element was designed and fabricated that corresponded to a linear phase increase along both the *x*- and y- axes. Fabrication parameters for this element were the same as for the first and are illustrated in Figure 4(b). The simulated and measured phase responses generated by the encoded element are represented in Figure 7. The measured results show the same overall response as the predicted phase response. As in the case of the first element, a random phase variation of ∼±15° is also present.

4. CONCLUSION

In this article, we described a design methodology for synthesizing DEs at millimeter wave frequencies using subwavelength cylindrical features. Our technique yields a single substrate element that generates complicated spatially varying phase responses. Our technique simplifies the fabrication process such that common methods such as laser or CNC drilling can be employed. By using subwavelength features our method also eliminates artifacts produced

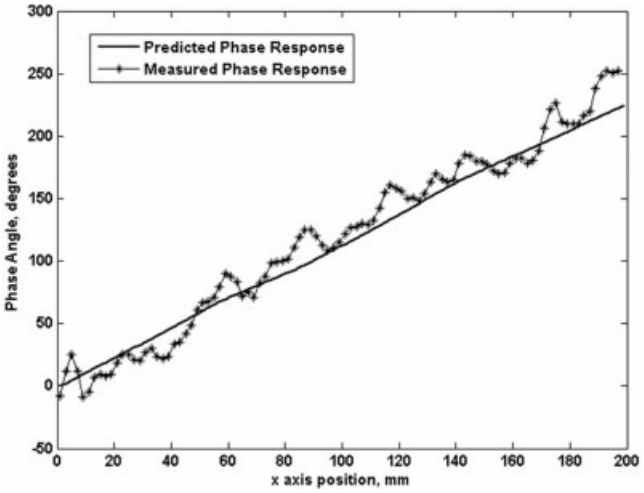

Figure 6 Experimental verses predicted results for the 1D linear phase ramp DE described in Figure 4(a)

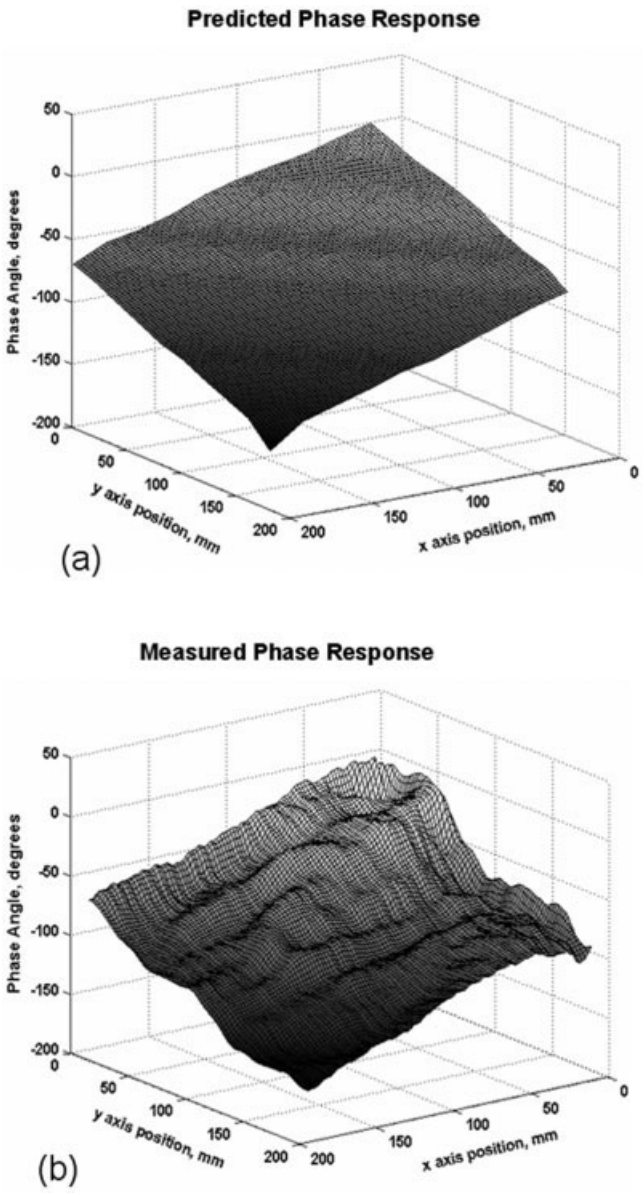

Figure 7 Experimental and predicted results for 2D linear phase ramp DE described in Figure 4(b)

by using larger binary-phase elements. We presented experimental results for two elements operating at 40 GHz that agreed reasonably well with our predictions of expected behavior.

REFERENCES

1. N. Nieuborg, A. Kirk, B. Morlion, H. Thienpont, and I. Veretennicoff, Polarization selective diffractive optical elements with an index-matching gap material, Appl Opt 36 (1997), 4681–4686.
2. L. Pajewski, R. Borghi, and G. Schettini, Design of binary grating with subwavelength features that acts as a polarizing beam splitter, Appl Opt 40 (2001), 5898–5905.
3. F. Xu, J. Ford, and Y. Fainman, Polarization-selective computer-generated holograms: Design, fabrication, and applications, Appl Opt 34 (1995), 256–266.
4. M.S. Mirotznik, D.M. Pustai, D.W. Prather, and J.N. Mait, Design of two-dimensional polarization-selective diffractive optical elements with form-birefringent microstructures, Appl Opt 43 (2004), 5947–5954.
5. P. Lalanne and J. Hugonin, High-order effective-medium theory of subwavelength gratings in classical mounting: Application to volume holograms, J Opt Soc Am A 15 (1998), 1843–1851.
6. E. Noponen and J. Turunen, Eigenmode method for electromagnetic synthesis of diffractive elements with three-dimensional profiles, J Opt Soc Am A 11 (1994), 2494–2502.
7. M.G. Moharam, D.A. Pommet, E.B. Grann, and T.K. Gaylord, Stable implementation of the rigorous coupled-wave analysis for surface-relief gratings: Enhanced transmittance matrix approach, J Opt Soc Am A 12 (1995), 1077–1084

A BAND-PASS FILTER CONSISTING OF TWO SUBSTRATE INTEGRATED WAVEGUIDE CAVITIES COUPLED BY AN APERTURE ON THEIR COMMON SIDE WALL

R. B. Hwang and C. W. Chang
Communication Engineering Department, National Chiao Tung University, Hsinchu, Taiwan, Republic of China

Received 24 January 2007

ABSTRACT: *In this article, we present a substrate-integrated waveguide-based band-pass filter with wide stop-band rejection property. This band-pass filter is made up of two substrate-integrated waveguide cavities, which couple to each other by an aperture on their common waveguide side wall. By using the empirical formula [19] for obtaining the equivalent rectangular waveguide dimensions, the substrate integrated waveguide structure could then be properly approximated by a closed rectangular waveguide. We employed the rigorous mode-matching method to analyze the electromagnetic boundary-value problem of the structure containing multiple discontinuities. In comparison with the conventional end-to-end coupled cavity filters, we found that our new side-wall-coupled cavity filter can suppress the second resonance frequency and therefore, provide a considerably wide rejection band. It is interesting to note that the suppression of the second resonance frequency can be achieved by properly shifting the second cavity in lateral direction. To explore its physical insight, the resonant modes in the substrate integrated waveguide cavities are carefully inspected for realizing the physical picture of wave process taking place in the two cavities system. In addition to the theoretical analysis, we have fabricated the filters and measured their scattering parameters. The good agreement between the theoretical and measured results validates the accuracy of numerical computation, and also shows the promising performance of the proposed filters.* © 2007 Wiley Periodicals, Inc.
Microwave Opt Technol Lett 49: 1884–1887, 2007; Published online in Wiley InterScience (www.interscience.wiley.com). DOI 10.1002/mop.22570

Key words: *band-pass filter; cavity; substrate integrated waveguide; resonator; periodic structures*

1. INTRODUCTION

Waveguide filters have been extensively used in microwave and millimeter wave engineering for many years [1–3]. Because of their high power-handling and high reliability, they were usually applied in deep-space and military radar applications. Recently, the post-wall waveguide technique [4–9], or the substrate integrated waveguide technique [10–19], was developed to fabricate an equivalent rectangular metallic waveguide on a low-loss microwave substrate. Such a class of waveguides has been proved [18] to be able to preserve the well-known advantages of conventional closed rectangular waveguide, such as high-Q factor. Be-